

Mimicking the TYC strategy: Weak Allee effects, and a “non” hyperbolic extinction boundary

Eric M. Takyi · Joydeb Bhattacharyya · Matthew Beauregard · Rana D. Parshad

the date of receipt and acceptance should be inserted later

Abstract The Trojan Y Chromosome strategy (TYC) is a genetic biocontrol strategy designed to alter the sex ratio of a target invasive population by reducing the number of females over time. Recently an alternative strategy is introduced, that mimics the TYC strategy by harvesting females whilst stocking males (Lyu et al., 2020) (FHMS). We consider the FHMS strategy, with a weak Allee effect, and show that the extinction boundary need *not* be hyperbolic. To the best of our knowledge, this is the first example of a non-hyperbolic extinction boundary in mating models, structured by sex. Next, we consider the spatially explicit model and show that the weak Allee effect is *both* sufficient and necessary for Turing patterns to occur. We discuss the applicability of our results to large scale biocontrol, as well as compare and contrast our results to the case with a strong Allee effect.

Keywords Trojan Y Chromosome · invasive species · weak Allee effect · extinction boundary · harvesting · Turing instability

Correspondence to: rparshad@iastate.edu

1 Introduction

Invasive aquatic species are an imminent threat to marine biodiversity. The rate of invasions due to alien species worldwide continues to rise (Havel et al., 2015a). Due to the various harmful effects of these species, their control is a paramount issue in ecology. Invasive species, upon effectively building up in another condition, can be hard to manage and the control expenses can get extreme. Gutierrez and Teem (Gutierrez and Teem, 2006) proposed an autocidal biocontrol TYC strategy to wipe out invasive species with XX/XY sex chromosomes via a constant release of YY males referred to as supermales. Exogenous sex hormones are utilized broadly to control sex in the aquaculture fishes. Male fish exposed to certain sex hormones can become feminized (Scott et al., 1989). Mating of a XY phenotypic female fish and a wild-type XY male fish produce supermale fish-bearing two Y chromosomes. YY supermales crossing to XX females yield all XY male offspring. The production of YY broodstock of Nile tilapia (Mair et al., 1997; Vera Cruz et al., 1999), yellow catfish (Liu et al., 2013), and brook trout (Schill et al., 2016a) has been proven successful by using TYC strategy. Further, for the production of YY supermales, supplying feminized YY supermales into an undesired population was proposed by Gutierrez and Teem (Gutierrez and Teem, 2006). There is a large literature on the TYC strategy

(Parshad and Gutierrez, 2010; Parshad, 2011; Gutierrez et al., 2013; Teem et al., 2014; Wang et al., 2014, 2016; Zhao et al., 2012; Parshad and Gutierrez, 2011; Gutierrez et al., 2012). Essentially,

Eric M. Takyi
Department of Mathematics, Iowa State University, Ames, IA 50011, USA.

Joydeb Bhattacharyya
Department of Mathematics, Karimpur Pannadevi College, Nadia, WB 741152, India.

Matthew Beauregard
Department of Physics, Engineering, and Astronomy, Stephen F Austin State University, Nacogdoches, TX 75962, USA.

Rana D. Parshad
Department of Mathematics, Iowa State University, Ames, IA 50011, USA.

- For the classical four species TYC model, given any initial condition for the invasive wild-type males and females, there exist initial conditions for the introduced feminised supermales, and a threshold introduction rate, such that for an introduction greater than this rate, extinction of the wild-type occurs (Gutierrez et al., 2012; Wang et al., 2014; Parshad and Gutierrez, 2011).
- The recent seminal work of Schill and collaborators (Schill et al., 2016a; Perrin, 2009; Havel et al., 2015b), makes it evident that biocontrol of TYC type rests purely on the introduction of the supermale - *not* feminized supermales, as these are still not in existence (and certainly not in mass production). Thus the three species TYC, with a one-time introduction of supermales, via the initial condition, is what occurs/is occurring in practice (Havel et al., 2015b).
- The three species TYC has been investigated in detail mathematically. The literature is rife with several results on well-posedness, and the long time dynamics of the system, under the assumptions of positive solutions (solutions that remain positive if they start from positive initial data) (Gutierrez et al., 2013; Parshad, 2011). Essentially, here again, a sufficient introduction of the supermale can always yield extinction. However, the three species TYC model is now known to be ill-posed - and solutions to the female component can blow-up in finite time (Parshad et al., 2019), if the introduction of supermales is too large.
- In order to circumvent the issues of blow-up or “unphysical” solutions, and due to the paucity of supermales, recent investigations into TYC type biocontrol have focused on (1) remodeling mating dynamics in TYC type models (Beauregard et al., 2020; Bhattacharyya et al., 2020) and (2) investigation models that “mimic” the TYC dynamics without using supermales such as using selective harvesting strategically (Lyu et al., 2020; Lyu, 2018).
- The consequences of a strong Allee effect on TYC type dynamics have also been recently investigated (Beauregard et al., 2020; Bhattacharyya et al., 2020). However, the impact of a *weak* Allee effect on the population dynamics in case of a TYC type strategy and/or a FHMS strategy is adopted, has not been investigated.

Harvesting in practice, is tricky to say the least. Although it has been used in invasive species management along with chemical and biological control measures, and can result in non-random removals of individuals from targeted populations (Britton et al., 2011; Myers et al., 2000). The potential selectivity of these methods therefore has strong ecological and evolutionary implications. Consequently, we suggest that Palkovacs et al.s (Palkovacs et al., 2018) framework could be applied to invasive species management. Indeed, harvest-driven trait changes in invasive species might induce unexpected and potentially counterproductive results that may not have been explicitly considered by ecosystem managers. The work of Lyu (Lyu, 2018; Lyu et al., 2020), demonstrates the potential for harvest as an effective strategy that can mirror the TYC strategy. In theory linear harvesting (and harvesting at various density dependent rates), seem to work better than a mimic of TYC where males are stocked and females harvested (FHMS) (Lyu, 2018; Lyu et al., 2020). However, the impact of Allee effects on the overall success or failure of such a class of strategies remains unexplored.

Allee effects are positive relationships between individual fitness and population density. These can be strong, where there is a threshold, below which the population growth rate is negative. They could also be weak, where the growth rate is always positive, but smaller at lower densities (Courchamp et al., 1999; Stephens and Sutherland, 1999). In the context of marine fishes, researchers observe that an Allee effect is significant at very low population size and with bias in sex ratio (Perälä and Kuparinen, 2017; Wedekind, 2012). Researchers (Neuenhoff et al., 2019; Perälä and Kuparinen, 2017) observed that extinction of Atlantic cod (*Gadus morhua*) in the southern Gulf of St. Lawrence and the depletion of Atlantic herring (*Clupea harengus*) population in the North Sea are due to predation-driven Allee effect. For a population with male-biased sex ratio would lead to difficulty in finding a mate, even for species that use powerful sex pheromones. Such skewed sex ratios fortify Allee effects on account of mating failure, prompting the risk of populace extinction. In sex structured (into male and female) population models, specially in fishes, having a weak Allee effect only on the female is quite feasible, as at low female densities, we would expect smaller clutch sizes - however a few males could fertilize a large number of females - so clutch sizes could still be large (Alonzo and Mangel, 2004).

The dynamics of sex structured two species mating models, even with the inclusion of Allee effects, is generically like Fig. 1 (a). There are typically two interior equilibria, one unstable (saddle) and one locally stable, also the extinction equilibrium is locally stable. The stable manifold of the saddle (separatrix) splits the phase space into two sections, delineated by the extinction boundary, also called the allee threshold or threshold manifold in the literature (Boukal and Berec, 2002; Jiang and Shi, 2009). If one picks initial data on one side of this curve, solutions tend to the stable interior equilibrium, and if one picks initial data on the other side of the boundary, solutions tend to the extinction equilibrium. Note, although the curve is seen to be of *hyperbolic*

shape (that is monotone with respect to initial conditions, in the phase space), the general shape of this curve, even in two species mating models, with or without Allee effects, is an open problem in ecology.

Also, by considering Allee effect in invasive fish population and a continued harvesting/stocking, the rarity of wild-type females would lead to difficulty in finding mates, and so the invasive fish population would eventually become locally extinct. However, it is not economically viable to harvest/stock indefinitely. Thus determining the time for terminating harvesting/stocking is critical as the wild-type invasive species would either go extinct or recover, such as in the absence of supermale invasive fish (Wang et al., 2014).

In the current manuscript we show that,

- Both a saddle-node and Homoclinic bifurcation can occur in the FHMS model with weak Allee effect via Lemma 9 and see Fig. 7. We show limit cycle dynamics is not possible without the weak Allee effect in place, via Lemma 4, however the weak Allee effect can lead to limit cycle dynamics, via Lemma 10.
- The FHMS model with a weak Allee effect, can exhibit an extinction boundary (Allee threshold) that is non-hyperbolic. Such dynamics can enable extinction, essentially for any initial data. This is completely different when a weak Allee effect is *not* in place. See Fig. 6. A non-hyperbolic extinction boundary is also possible via a strong Allee effect, see Fig. 8, but the “bending” of the boundary is not as pronounced as in the weak Allee effect case.
- We show when/if harvesting/stocking can be terminated at certain finite time, and when the population of invasive fish is below some threshold, to yield extinction. See Figs. 4 - 5.
- We consider the spatially explicit FHMS model with weak Allee effect. We show that the weak Allee effect can cause Turing instability, and impossibility without it, via Lemma 11, and Theorem 4.
- We discuss the implications of our results to biocontrol, via these strategies.

2 Background

Here we recap the basic TYC and FHMS models as presented in (Lyu, 2018) and (Parshad and Gutierrez, 2010).

2.1 The TYC Model

In the TYC strategy, supermales (S) of the invasive species with two YY Chromosomes, are introduced into the wild-type invasive fish population having wild-type males (M) and females (F). The rate of injection of supermale invasive fish is taken as μ_0 (population time^{-1}). The reproduction rate of wild-type invasive fish species due to the interactions between male and female wild-type invasive fish species is β_1 (population $^{-1}$ time^{-1}), whereas the reproduction rate of wild-type invasive fish due to the interactions between wild-type female invasive fish and supermale invasive fish is β_2 (population $^{-1}$ time^{-1}). The death rates of wild-type and the supermale invasive fish are taken as δ_1 (time^{-1}) and δ_2 (time^{-1}) respectively. The carrying capacity of the system is K_1 (population), and the logistic term $L = 1 - \frac{F+M+S}{K_1}$ is used to constrain the invasive fish population. The equations describing the TYC model are:

$$\begin{aligned}\frac{dF}{dT} &= \frac{1}{2}\beta_1 F M L - \delta_1 F \\ \frac{dM}{dT} &= F \left(\frac{1}{2}\beta_1 M + \beta_2 S \right) L - \delta_1 M \\ \frac{dS}{dT} &= \mu_0 - \delta_2 S,\end{aligned}\tag{1}$$

where $F(0) \geq 0$, $M(0) \geq 0$ and $S(0) \geq 0$.

2.2 Existence and stability of equilibria when $\mu_0 = 0$

We refer the reader to (Wang et al., 2014) for detailed analysis on the existence and stability of equilibria to system (1). The equilibria to system (1) after nondimensionalization are $E_0 = (0, 0)$ and $E_{1,2} = (f_{\pm}^*, m_{\pm}^*)$ with $f^* = m^*$ where

$$f_{\pm}^* = \frac{1}{4} \left(1 \pm \sqrt{1 - \Phi} \right), \text{ where } \Phi = \frac{8}{\rho}.$$

We recap some standard results on the model (Wang et al., 2014),

Theorem 1 . If $\Phi < 1$,

- (i) the extinction state E_0 is locally stable.
- (ii) the equilibrium point E_1 is locally stable.
- (iii) the equilibrium point E_2 is locally unstable.

Remark 1 . When $\rho = 8$, the two interior equilibrium points E_1 and E_2 collide with each other giving rise to a saddle-node bifurcation.

2.3 The FHMS Model

A key issue in the implementation of the TYC strategy is the production of supermales. Estrogen-induced feminization of the wild-type male fish has often proven inefficient to obtain sex-reversed XY physiological females. In such a situation, we can implement a sex-skewing strategy by removing a fraction of wild-type females by means of harvesting whilst adding in the wild-type males by means of stocking. This strategy is called female harvesting male stocking (FHMS), first proposed by Lyu (Lyu, 2018; Lyu et al., 2020).

For the FHMS model described below, the primary sex ratio in offspring is denoted by r ($0 < r < 1$). The harvesting rate of females and the stocking rate of the males are denoted by h_F and s_M respectively. Also, we assume that $0 \leq s_M < \delta$. The equations describing the FHMS system are:

$$\begin{aligned} \frac{dF}{dT} &= r\beta FML - (\delta + h_F)F \\ \frac{dM}{dT} &= (1-r)\beta FML + (s_M - \delta)M, \end{aligned} \quad (2)$$

where $F(0) \geq 0$ and $M(0) \geq 0$.

In order to reduce the number of parameters, we introduce dimensionless variables

$$f = \frac{F}{K_1}, \quad m = \frac{M}{K_1}, \quad t = T\delta,$$

and the dimensionless parameters

$$\alpha = \frac{\beta K_1}{\delta}, \quad h = \frac{h_F}{\delta}, \quad s = \frac{s_M}{\delta}.$$

With these substitutions, the equations describing the system become:

$$\begin{aligned} \frac{df}{dt} &= r\alpha f m (1 - f - m) - (1 + h)f \equiv F_1(f, m) \\ \frac{dm}{dt} &= (1 - r)\alpha f m (1 - f - m) + (s - 1)m \equiv F_2(f, m), \end{aligned} \quad (3)$$

where $f(0) \geq 0$ and $m(0) \geq 0$.

We recap the following results (Lyu, 2018; Lyu et al., 2020),

Lemma 1 . If $f(0)$ and $m(0)$ are positive, then all possible solutions of the system (3) are non-negative.

Lemma 2 . All the solutions of the system (3) are contained in some bounded subset in the plane

$$\left\{ (f, m) \in \mathbf{R}^2 : f \geq 0, \quad m \geq 0 \right\}.$$

2.4 Equilibria and their stability

The equilibria and stability analysis of system (3) are presented in Appendix A. We state some results on (3) that were not shown in (Lyu et al., 2020),

Lemma 3 . For $h_* < h < h^*$, the invasive species get eliminated from the system (3) via saddle-node bifurcation when s is decreased through $s = s^*$.

Proof . At $s = s^*$, we have $f^* = \frac{1}{2(1+\mu)}$ where $\mu = \frac{(1-r)(1+h)}{r(1-s)}$ and so $\text{Det}(J^*)|_{s=s^*} = 0$, where J^* is the Jacobian of system (3). Since $\text{Tr}(J_i^*) < 0$, it follows that J_i^* has a simple eigenvalue at $s = s^*$.

Let $F(f, m; s) = (F_1 \ F_2)^T$ and V and W are the eigenvectors corresponding to the zero eigenvalue for $J^*|_{s=s^*}$ and $J^{*T}|_{s=s^*}$ respectively. Then we have $F_s(f, m; s) = \left(0 \ \frac{\mu}{2(1+\mu)}\right)^T$, $U = (1 \ \mu)^T$ and $V = \left(1 \ \frac{r}{\mu(1-r)}\right)^T$. This gives $V^T F_s(E_i^*; s^*) = \frac{r}{2(1+\mu)(1-r)} \neq 0$ and $V^T [D^2 F(E_i^*; s^*)(U, U)] = -r\alpha(1+\mu) \neq 0$. Therefore, by Sotomayor's theorem (Perko, 2013) it follows that the system (3) undergoes a saddle-node bifurcation at E_i^* when s crosses s^* .

Lemma 4 . System (3) has no limit cycles.

Proof . We use the Dulac theorem to show the non-existence of limit cycles in (3). Let us consider the Dulac function

$$\Psi(f, m) = \frac{1}{fm} \quad (4)$$

where $f \neq 0$ and $m \neq 0$. Then,

$$\begin{aligned} \frac{\partial(F^1 \Psi)}{\partial f} + \frac{\partial(F^2 \Psi)}{\partial m} &= \frac{\partial}{\partial f} \left(r\alpha(1-f-m) - \frac{1+h}{m} \right) + \frac{\partial}{\partial m} \left((1-r)\alpha(1-f-m) + \frac{s-1}{f} \right) \\ &= -r\alpha - (1-r)\alpha \\ &= -\alpha < 0. \end{aligned}$$

Hence the system (3) has no limit cycles. This completes the proof.

Lemma 5 . If $h = 0 = s$, then system (3) has no limit cycles.

Proof . Suppose $h = 0 = s$ in system (3). We use the Dulac theorem again and consider the Dulac function in Eq.(4). Then,

$$\frac{\partial(F^1 \Psi)}{\partial f} + \frac{\partial(F^2 \Psi)}{\partial m} = \frac{\partial}{\partial f} \left(r\alpha(1-f-m) - \frac{1}{m} \right) + \frac{\partial}{\partial m} \left((1-r)\alpha(1-f-m) - \frac{1}{f} \right) = -r\alpha - (1-r)\alpha = -\alpha < 0.$$

Hence the system (3) has no limit cycles for $h = 0 = s$. This completes the proof.

3 The FHMS Model with a weak Allee Effect

We modify the system (3) by considering Allee effect in the population. The equations describing the FHMS system with a weak Allee effect are given by:

$$\begin{aligned} \frac{dF}{dT} &= r\beta F^2 ML - (\delta + h_F)F \\ \frac{dM}{dT} &= (1-r)\beta F^2 ML + (s_M - \delta)M, \end{aligned} \quad (5)$$

where $F(0) \geq 0$ and $M(0) \geq 0$.

We introduce dimensionless variables

$$f = \frac{F}{K_1}, \quad m = \frac{M}{K_1}, \quad t = T\delta,$$

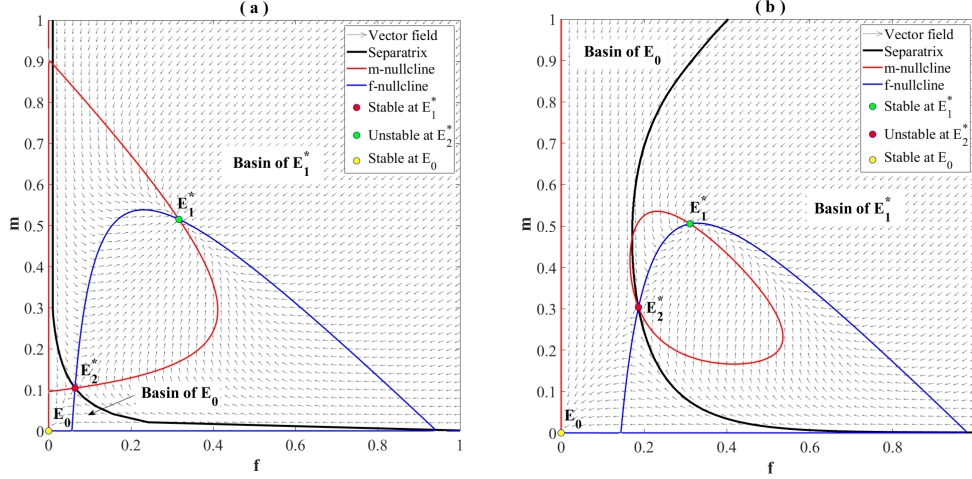


Fig. 1 The separatrix divides the phase plane into the regions of extinction and recovery for the (a) FHMS system (3) without Allee and (b) FHMS system (6) with weak Allee

and the dimensionless parameters

$$\alpha = \frac{\beta K_1^2}{\delta}, \quad h = \frac{h_F}{\delta}, \quad s = \frac{s_M}{\delta}.$$

With these substitutions, the equations describing the system become:

$$\begin{aligned} \frac{df}{dt} &= r\alpha f^2 m(1-f-m) - (1+h)f \equiv \bar{F}_1(f, m) \\ \frac{dm}{dt} &= (1-r)\alpha f^2 m(1-f-m) + (s-1)m \equiv \bar{F}_2(f, m), \end{aligned} \quad (6)$$

where $f(0) \geq 0$ and $m(0) \geq 0$.

Lemma 6 . If $f(0)$ and $m(0)$ are positive, then all possible solutions of the system (6) are non-negative.

Proof . We have $f(t) = f(0)e^{\int_0^t \phi_1(f, m; \tau) d\tau}$ and $m(t) = m(0)e^{\int_0^t \phi_2(f, m; \tau) d\tau}$, where $r\{m\phi_2(f, m; t) + 1 - s\} = (1-r)\{f\phi_1(f, m; t) + 1 + h\}$. Here $\phi_1 = r\alpha f m(1-f-m) - (1+h)$ and $\phi_2 = (1-r)\alpha f^2(1-f-m) + (s-1)$.

This implies, all solutions of (6) remain within $\{(f, m) \in \mathbf{R}^2 : f \geq 0, m \geq 0\}$ starting from an interior point of it. Therefore, $\mathbf{R}_+^2 = \{(f, m) \in \mathbf{R}^2 : f > 0, m > 0\}$ is an invariant region, and as long as $f(t) > 0$ and $m(t) > 0$ for all t , the local existence and uniqueness properties hold in \mathbf{R}_+^2 . We now prove that the solutions of (6) with initial values in \mathbf{R}_+^2 are bounded, so that the system (6) is biologically meaningful.

Lemma 7 . All the solutions of the system (6) are contained in some bounded subset in the plane

$$\{(f, m) \in \mathbf{R}^2 : f \geq 0, m \geq 0\}.$$

The proof is shown in section B.1.

3.1 Equilibria and their stability

System (6) has the nullclines $\bar{F}_i = 0$ ($i = 1, 2$). Solving these nullclines yields the following equilibria:

- (i) Invasive fish-free equilibrium $E_0 = (0, 0)$ exists always and is locally asymptotically stable (as $s < 1$).
- (ii) coexistence equilibria $E_i^* = (f_i^*, \mu f_i^*)$, where $\mu = \frac{(1-r)(1+h)}{r(1-s)}$ and f_i^* is a positive root of the equation

$$G(f) \equiv f^3 - \frac{1}{1+\mu}f^2 + \frac{1+h}{r\alpha\mu(1+\mu)} = 0.$$

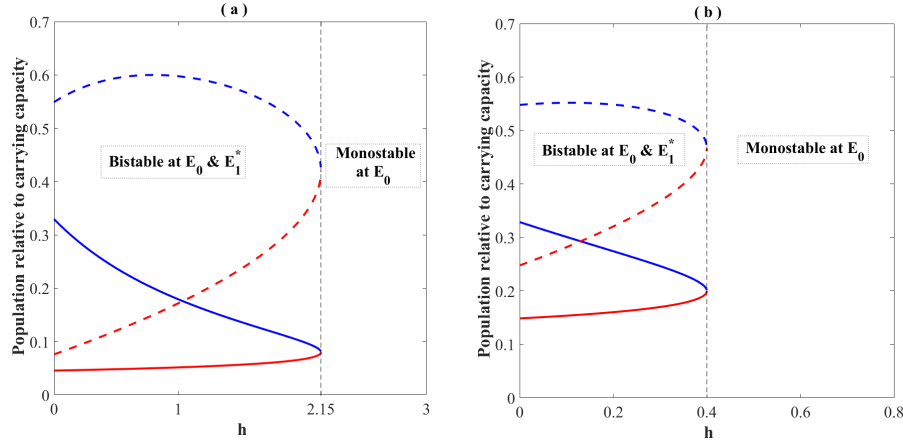


Fig. 2 Bifurcation diagrams of the (a) FHMS model without Allee effect (3) and (a) FHMS model with weak Allee effect (6), where h as the bifurcation parameter (XX and XY are in solid and dotted curves respectively). The stable and unstable equilibrium are represented by the blue curve and the red curve, respectively

The stability of system (6) is determined by using eigenvalue analysis of the Jacobian matrix evaluated at the appropriate equilibrium. The eigenvalues of the Jacobian matrix ($J(E_0)$) of the system (6) at E_0 are $s - 1$ and $-(1 + h)$. Since $0 \leq s < 1$, all the eigenvalues of $J(E_0)$ are negative. This gives the following lemma:

Lemma 8 . *The invasive fish-free equilibrium E_0 is always locally asymptotically stable.*

The Jacobian of the system (6) evaluated at E_i^* is given by

$$J_i^* = \begin{pmatrix} r\alpha\mu f_i^{*2}(1 - 2f_i^* - \mu f_i^*) & r\alpha f_i^*(1 - f_i^* - 2\mu f_i^*) \\ (1 - r)\alpha\mu f_i^{*2}(2 - 3f_i^* - 2\mu f_i^*) & -(1 - r)\alpha\mu f_i^{*3} \end{pmatrix}.$$

The system (6) is locally asymptotically stable at E_i^* if and only if $\text{Tr}(J_i^*) < 0$ and $\text{Det}(J_i^*) > 0$.

From Fig. 3 it is observed that as the harvesting rate (h) is increased, the female-male gender ratio drops significantly. Once h crosses some critical threshold value, there leads to a sudden change of transition from stable coexistence state to invasive fish-free state (cf. Fig. 2). Therefore, it is necessary to study the behaviour of the system (6) by considering h as a bifurcation parameter.

Lemma 9 . *The invasive species get eliminated from the system (6) via saddle-node bifurcation when h is increased through $h = h^*$.*

The proof is given in the appendix section B.2.

Lemma 10 . *Consider the Jacobian of system (6). If the following hold*

- (i) $\text{Tr}(J_i^*)|_{E_1^*} = 0$,
- (ii) $\text{Det}(J_i^*)|_{E_1^*} > 0$,
- (iii) $\frac{d}{ds}(\text{Tr}(J_i^*))|_{E_1^*} \neq 0$ at $s = s_{hf}$,

then the system (6) exhibits periodic oscillation via a Hopf bifurcation when s is increased through $s = s^$.*

The proof is given in the appendix section B.3.

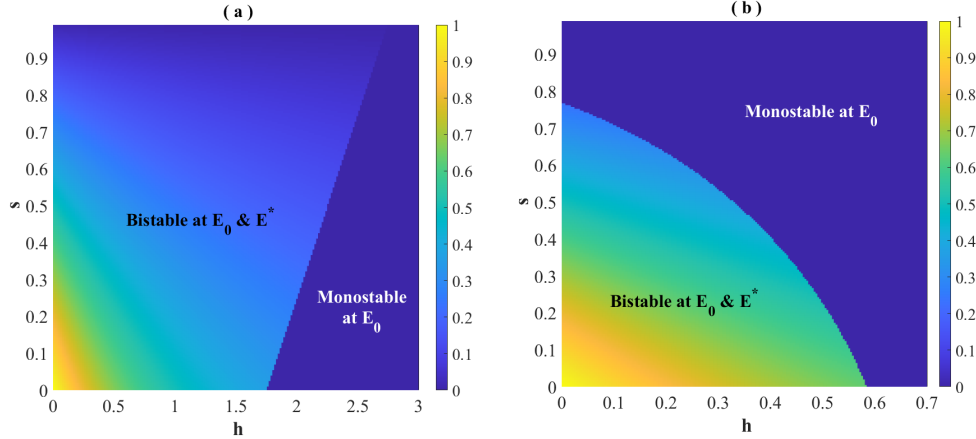


Fig. 3 The changes in the female-male gender ratio with the changes in the scaled harvesting rate (h) and the scaled stocking rate (s) for the (a) FHMS model without Allee effect (3) and (b) FHMS model with weak Allee effect (6)

3.2 Intermediate Harvesting

As a result of the Allee effect in the invasive fish population, with the harvesting rate $h \geq h^*$, the eradication of invasive fish can be successfully achieved by stopping the harvesting and stocking once the female invasive fish population fall below some threshold value. The minimum number of females needed for its survival would give the minimum time of continuous harvesting and stocking in order to eradicate invasive fish species. Once the harvesting and stocking of the invasive fish are stopped, the dynamics of the system will be governed by system (6) with $h = 0$ and $s = 0$. Each of these systems has a stable fish-free boundary equilibrium. In the phase plane, once the solution trajectories enter the basin of attraction of the boundary equilibrium, the fish species become extinct. Determining the threshold of the female fish population is critical as after discontinuing the harvesting and stocking, the invasive fish species would either go extinct or recover.

It has been observed that with the female-harvesting rate at h^* and with different initial sex ratios, the minimum threshold female population for survivability lies in between 0.1 and 0.15 (cf. Fig. 4). It is seen that at a given supply rate, the minimum harvesting time of female invasive fish varies with the initial population densities of invasive fish. While the minimum time for the continuous harvesting of females increases with the initial population of equal sex ratio (cf. Figs. 4(a) & 4(b)), population densities initially sex-skewed towards males require less harvesting time than the population sex-skewed towards females (cf. Figs. 4(c) & 4(d)). For $h = 0 = s$ and $h = h^*$, let the separatrices of extinction and recovery of the invasive fish population be in the form $f = \Gamma_h^0(m)$ and $f = \Gamma_h^*(m)$ respectively. Then the regions of extinction for $h = 0 = s$ and $h = h^*$ in the fm -plane are given by:

$$R_h^0 = \{(f, m) \in R^2 : 0 \leq f \leq \Gamma_{hs}^0(m), 0 \leq m \leq 1\} \text{ and } R_h^* = \{(f, m) \in R^2 : 0 \leq f \leq \Gamma_h^*(m), 0 \leq m \leq 1\} \text{ respectively.}$$

The eradication strategy would be to discontinue harvesting and stocking of invasive fish once the invasive fish population enters the region $R_h^0 \cap R_h^*$ (cf. Fig. 5).

At a given initial population density of the invasive fish species and the harvesting rate of female invasive fish at its minimum admissible value h^* , this technique will give the least possible continuous harvesting or (and) stocking time in order to eliminate the invasive fish species from the system. Fig. 5 gives the minimum continuous harvesting or (and) stocking time of the invasive fish for the complete removal of the invasive fish population with different initial population densities.

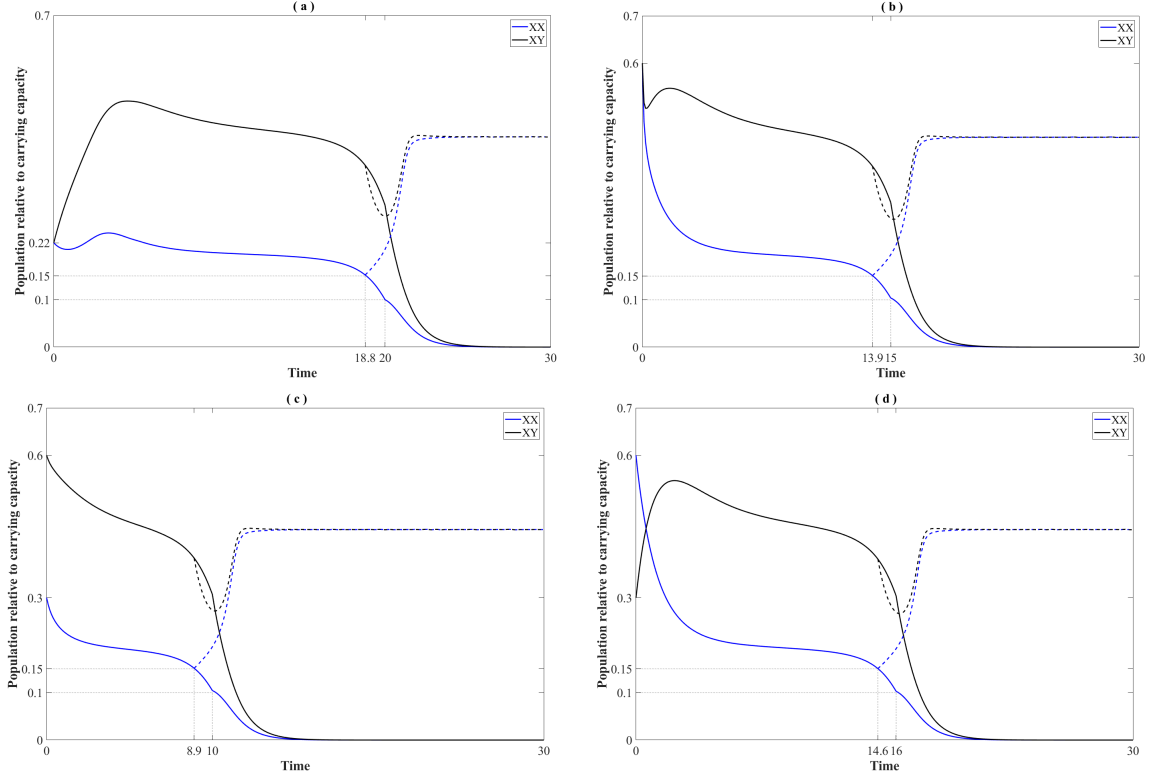


Fig. 4 The time for extinction and recovery of invasive fish population with (a) low and (b) high initial population densities at 1 : 1 sex-ratio. Time for extinction and recovery of invasive fish population with initial wild-type population sex-ratio is (c) skewed towards males ($f(0) : m(0) = 1 : 2$) and (d) skewed towards females ($f(0) : m(0) = 2 : 1$). The harvesting rate of the female species is kept at its minimum admissible value h^* for eradication. The plots for extinction and recovery are represented by solid and dashed lines, respectively

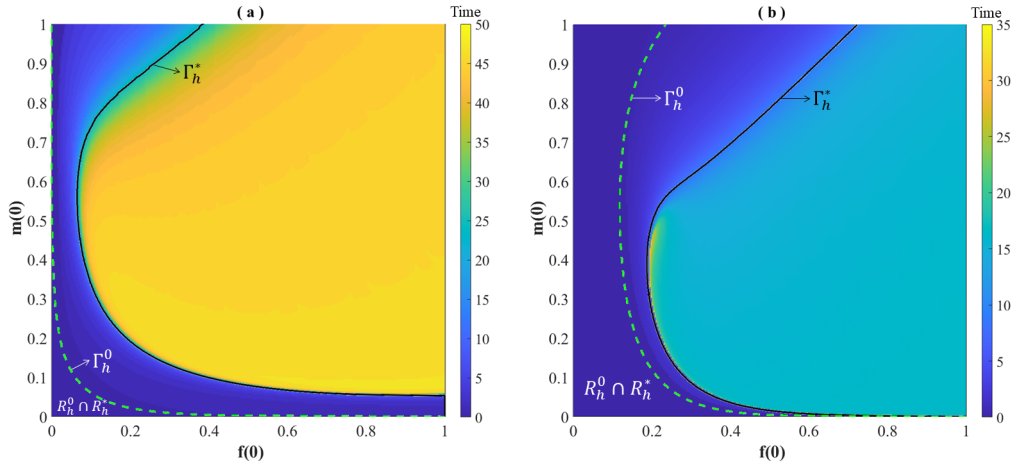


Fig. 5 The minimum continuous harvesting and stocking time for the elimination of the invasive fish population with different initial population densities for the (a) FHMS system (3) without Allee and (b) FHMS system (6) with weak Allee. The separatrices for the systems with $h = h^*$ and $h = 0 = s$ are denoted by the curves Γ_h^* and Γ_h^0 respectively

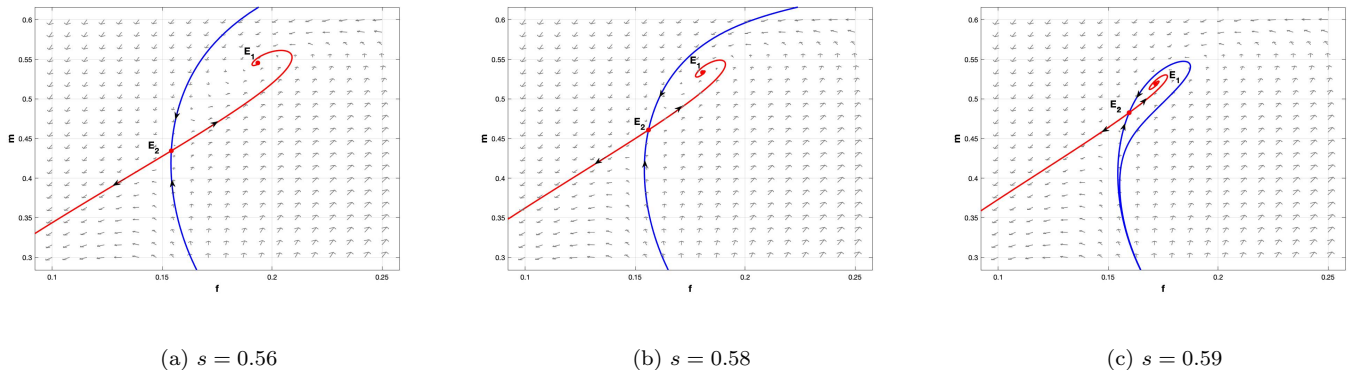


Fig. 6 Here we see the dynamics of a weak Allee effect in place. We notice in (a) and (b) the phase is split into two regions by the separatrix/stable manifold of the saddle E_2 , with a large proportion of the initial data going to the recovery state E_1 , which is a spiral sink. (c) shows this can change, as we vary the stocking parameter s - the unstable manifold of E_2 can loop around E_1 , and eventually lead to a homoclinic orbit. The other parameter values are $r = 0.5, \alpha = 90, h = 0.24$

3.3 The Extinction Boundary

As mentioned earlier, the dynamics of sex structured two species mating models is generically like Fig. 1 (a). The stable manifold of the saddle (separatrix) divides the phase space, delineated by an extinction boundary, also called “Allee” threshold (when there are Allee effects included) (Boukal and Berec, 2002) or threshold manifold (Jiang and Shi, 2009). If one picks initial data on one side of the boundary, solutions tend to the stable interior equilibrium, and if on the other side, solutions tend to the extinction equilibrium. Note, it is always seen to be of *hyperbolic* shape (monotone w.r.t initial data). The literature is rife with examples of such mating models - where the extinction boundary always turns out to be hyperbolic (Courchamp et al., 2008; Boukal and Berec, 2002; Berec, 2004). Notably, Schreiber rigorously proved, that there exists a hyperbolic extinction boundary in the case that certain sufficient conditions on the system concerned are met (Schreiber, 2004) - strong monotonicity of the system being one of them. The results have been proved for general monotone systems as well (Smith and Thieme, 2001; Hirsch and Smith, 2006). In the event that the sufficient conditions of (Schreiber, 2004) are not met, the shape of the Allee threshold remains an open problem (Berec, 2004). In particular, in cases where a strong Allee effect has been introduced into TYC type mating dynamics, we still see a hyperbolic extinction boundary (Beauregard et al., 2020; Bhattacharyya et al., 2020), but this might be due to a lesser exploration of the parameter space.

Remark 2 . Consider a population system $\dot{x} = xG(x)$, where $x = (f, m)$. Then (Schreiber, 2004), requires that if $\exp(G(0, 0))$ is primitive (and some other technical conditions are met), then that implies that there exists a hyperbolic extinction boundary. In our case,

$$\exp(G(0, 0)) = \begin{pmatrix} \exp(-(1+h)) & 0 \\ 0 & \exp(s-1) \end{pmatrix}. \quad (7)$$

This is not primitive. Hence the shape of the exact extinction boundary in our case is unknown.

We show, via numerical simulation that the FHMS model with weak Allee effect, can exhibit interesting dynamics in that the extinction boundary may not be hyperbolic. In Fig. 6, we increase the stocking parameter s and observe that the extinction boundary changes from the standard hyperbolic shape, to a loop. In Fig. 7 we see a limit cycle form, collide with the saddle, the stable manifold, the unstable manifold and form a homoclinic orbit - via a homoclinic bifurcation.

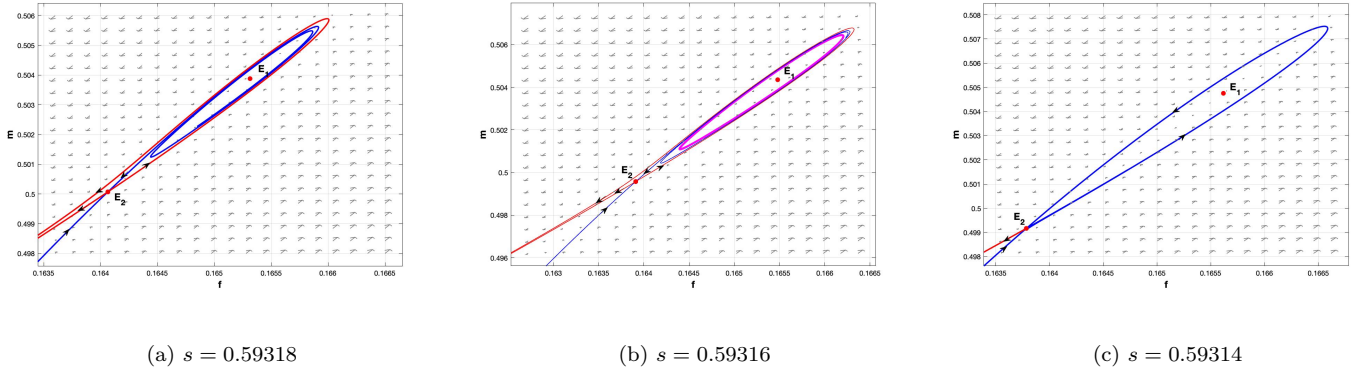


Fig. 7 Phase space showing the path to the occurrence of a Homoclinic orbit for different stocking s values. The stable and unstable manifolds are colored blue and red respectively. The unstable limit cycle is colored pink. The parameter values are $r = 0.5, \alpha = 90, h = 0.24$. E_1 is spiral source at $s = 0.59318$, it gains stability through a subcritical Hopf bifurcation, resulting in the occurrence of an unstable limit cycle at $s = 0.59316$. The limit cycle grows at s is decreased further, and at $s = 0.59314$ it collides with the stable and unstable manifold and the saddle E_2 to form a homoclinic orbit

3.4 The case of strong Allee effect

Consider the scaled mating model without female harvesting and male stocking, but with a strong Allee effect

$$\begin{aligned} \frac{df}{dt} &= r\alpha m(f - A)(1 - f - m) - f \\ \frac{dm}{dt} &= r\alpha m(f - A)(1 - f - m) - m, \end{aligned} \quad (8)$$

where f, m are the female and male population size and A is the Allee threshold. Our aim is to investigate the extinction boundary as the Allee threshold A is varied. What we notice is that for small Allee thresholds, $A < \approx 0.3$, the extinction boundary is non-hyperbolic again, see Fig. 8. However, it returns to a hyperbolic shape once the Allee threshold is increased past 0.7.

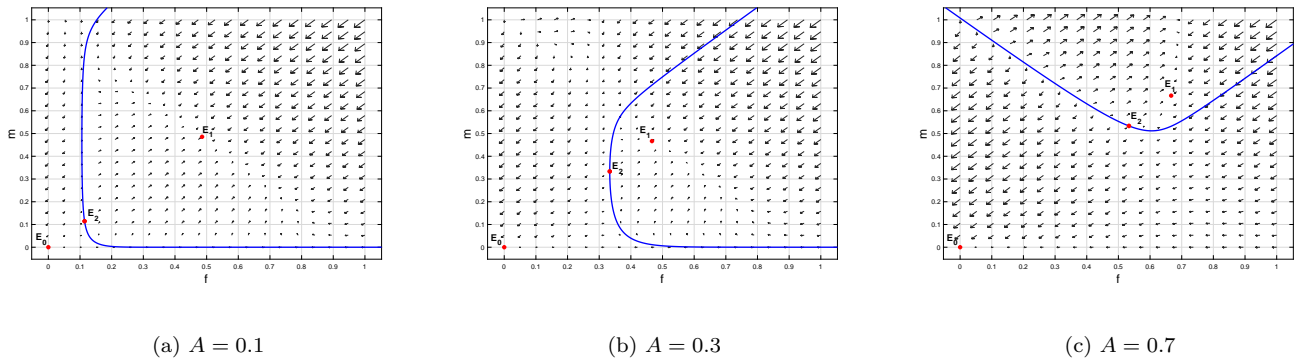


Fig. 8 Here we observe the dynamics with a strong Allee effect in place via (8). The phase space of scaled mating model split into two regions by separatrix with different Allee thresholds. One can see that the extinction boundary bends, and is thus non-hyperbolic. Although a complete loop is not formed such as Fig. 6. Also note increasing the Allee threshold (when a strong Allee effect is present) typically results in initial data from a larger region of the phase space, going to extinction. Here we notice an opposite effect, wherein increasing the Allee threshold from 0.3 to 0.7, causes a larger portion of the initial data to go to the recovery state. The parameter values $r = 0.5$ and $\alpha = 180$ are used in the simulation

4 Turing Instability

Species disperse due to various factors such as search for food, mates, to look for resources as well as to avoid predators or competitors [Murray \(2001\)](#). Thus there is a rich history of spatially explicit models in mathematical biology [Okubo \(2013\)](#). With a spatially explicit model, just as with an ODE model, one can analyze the steady states. Herein, various additional dynamics are possible - in particular the states might not be homogenous in space. This could be indicative of the populations spreading and/or living in varying densities in a spatial domain. One might see the phenomenon of Turing instability per se [Murray \(2001\)](#), whereby large differences in the diffusion coefficients can destabilize the spatially homogenous steady state. In this section, we explore the possibility of a Turing instability in systems (3) and (6) by including a spatial component.

4.1 Spatially explicit FHMS

We consider the system,

$$\begin{aligned}\frac{\partial f}{\partial t} &= d_1 \Delta f + r \alpha f m (1 - (f + m)) - (1 + h) f \\ \frac{\partial m}{\partial t} &= d_2 \Delta m + (1 - r) \alpha f m (1 - (f + m)) + (s - 1) m,\end{aligned}\tag{9}$$

where $f(x, t), m(x, t)$ are functions of both the spatial variable x and time t . Δ is the standard Laplacian operator, representing the diffusion of the species in space. We prescribe Neumann boundary conditions $f_x = 0, m_x = 0$ which represents no flux of the species into or out of the spatial domain. We also impose positive initial conditions $f(x, 0) > 0, m(x, 0) > 0$. The positive constants d_1 and d_2 are the diffusion coefficients. We choose a suitable domain $\Omega = [0, \pi]$ for our numerical simulations.

4.2 Spatially explicit FHMS with weak Allee effect

Consider the system

$$\begin{aligned}\frac{\partial f}{\partial t} &= d_{11} \Delta f + r \alpha f^2 m (1 - (f + m)) - (1 + h) f \\ \frac{\partial m}{\partial t} &= d_{22} \Delta m + (1 - r) \alpha f^2 m (1 - (f + m)) + (s - 1) m,\end{aligned}\tag{10}$$

subject to Neumann boundary conditions $f_x = 0, m_x = 0$ and positive initial conditions $f(x, 0) > 0, m(x, 0) > 0$. The positive constants d_{11} and d_{22} are the diffusion coefficients. Similar to system (9), we choose the domain $\Omega = [0, \pi]$.

Theorem 2 . (Turing instability condition) Let (f^*, m^*) be a non-trivial positive homogeneous steady state. For any given set of parameters, if the Jacobian $J_i^* = \begin{pmatrix} J_{11} & J_{12} \\ J_{21} & J_{22} \end{pmatrix}$ of the reaction terms evaluated at (f^*, m^*) and the diffusion constants d_1, d_2 satisfy

$$J_{11} + J_{22} < 0,\tag{11}$$

$$J_{11} J_{22} - J_{21} J_{12} > 0,\tag{12}$$

$$d_2 J_{11} + d_1 J_{22} > 0,\tag{13}$$

$$(d_2 J_{11} + d_1 J_{22})^2 - 4 d_1 d_2 (J_{11} J_{22} - J_{21} J_{12}) > 0,\tag{14}$$

then in the absence of diffusion, (f^*, m^*) is linearly stable and linearly unstable in the presence of diffusion.

We refer the reader to [\(Murray, 2001\)](#) for a more detailed derivation of the conditions necessary and sufficient for the occurrence of Turing instability.

Theorem 3 . (Necessary condition for Turing instability) A necessary condition for the occurrence of Turing instability is either $J_{11} < 0, J_{22} > 0$ or $J_{11} > 0, J_{22} < 0$ of the Jacobian J_i^* .

Lemma 11 . System (9) does not exhibit Turing instability.

Proof . Clearly, $J_{11} < 0, J_{22} < 0$ in the Jacobian J_i^* of the reaction terms in system (9) (that is, the Jacobian of system (3) seen in Appendix A) and hence does not meet the necessary condition for the occurrence of Turing instability. Hence proof.

In this section, we use the following set of parameters for all numerical experiments:

$$r = 0.5, \alpha = 90, h = 0.24, s = 0.5931. \quad (15)$$

Theorem 4 . System (10) *exhibits Turing instability*.

Proof . Consider the parameter set in Eq.(15). With these values, a homogeneous steady state of system (10) is $(f^*, m^*) = (0.165847, 0.505407)$. The Jacobian evaluated at (f^*, m^*) yields $J_i^* = \begin{pmatrix} 0.614441 & -0.218659 \\ 1.85444 & -0.625559 \end{pmatrix}$.

Clearly, $J_{11} = 0.614441 > 0, J_{22} = -0.625559 < 0$ of J_i^* meets the necessary condition for Turing instability occurrence. The eigenvalues of J_i^* are $\lambda_1 = -0.00555889 + 0.145224i$ and $\lambda_2 = -0.00555889 - 0.145224i$. The real parts of λ_1, λ_2 are both negative and hence the steady state (f^*, m^*) is locally stable. Simple calculations show that, $J_{11} + J_{22} = -0.011118 < 0, J_{11}J_{22} - J_{21}J_{12} = 0.0211209 > 0, d_2J_{11} + d_1J_{22} = 0.0614 > 0$ and $(d_2J_{11} + d_1J_{22})^2 - 4d_1d_2(J_{11}J_{22} - J_{21}J_{12}) = 0.00376685 > 0$. All conditions for the occurrence of Turing instability have been met. Hence proof.

We define a small perturbation around the positive homogeneous steady state as

$$\begin{aligned} f &= f^* + \alpha_1 \sin^2(nx) \\ m &= m^* + \alpha_2 \sin^2(nx), \end{aligned} \quad (16)$$

where $\alpha_1, \alpha_2, n \in \mathbf{R}$.

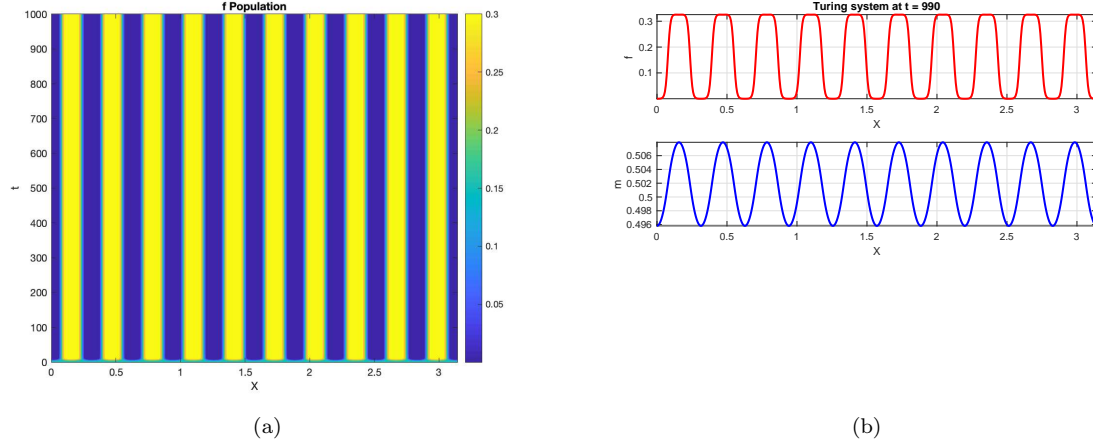


Fig. 9 Turing instability in FHMS with weak Allee in system (10). (a) Turing patterns in female population. (b) Spatial profile of female and male populations after simulation is run longer ($t = 1000$). The diffusion constants are $d_{11} = 0.0001, d_{22} = 0.1$. We give the spatially positive homogeneous steady state a small perturbation as in Eq.(16) where $\alpha_1 = 0.01, \alpha_2 = 0.01$ and $n = 10$

5 Discussion and Conclusion

In this work, we investigate models that mimic the TYC strategy, such as the FHMS models initiated in (Lyu, 2018; Lyu et al., 2020). These are critical research directions in biocontrol, given that supermale production has been successfully achieved by only one group in the US (Perrin, 2009; Schill et al., 2016a), and the feminised supermale is still not in existence. Furthermore, given strong evidence of weak Allee effects at low population densities, it is important to incorporate them into models of biocontrol, particularly in those which attempt

to reduce the female population density - as a means of driving the overall population to extinction. Here, the weak Allee effect is apt, because it works on positive density dependence, and populations still grow at low densities, only slower. So it is truly “weaker” than a strong Allee effect, which would imply negative density dependence below the Allee threshold.

The interplay of the harvesting and stocking with the weak Allee effect is important for bi-stability. To elucidate, let us focus on Fig. 3. Herein in (a), there is no weak Allee effect. At a harvesting level of $h = 0.5$, one can increase stocking unboundedly, but the system will remain bi-stable. However if we observe (b), where there is a weak Allee effect, at $h = 0.5$, if one increases stocking above $s = 0.25$, we have only mono stability, and all initial conditions go to the extinction state. This raises the question of what exactly is the extinction boundary in the FHMS system vs the one in the FHMS system with weak Allee effect.

To this end, we have derived various results with important implications for control. We show that the FHMS model with weak Allee effect in conjunction with harvesting and stocking, can produce a non-hyperbolic extinction boundary, see Fig. 6. This, to the best of our knowledge, is the first example of such a boundary in 2 species structured, mating models. The implication for control (for parameter choices say in Fig. 6) is that in situations, where we raise the stocking by just 1%, we can get essentially any initial condition, driven to the extinction state. It is important to note, that the weak Allee effect, and harvesting and stocking pressures are not exclusively responsible for a non-hyperbolic shaped extinction boundary - one can see this shape or “bending” even when a strong Allee effect is present, see Fig. 8. Although a complete loop is not formed such as Fig. 6. This result is counter intuitive, in that typically increasing the Allee threshold (when a strong Allee effect is present) results in initial data from a larger region of the phase space, going to extinction - but the opposite is observed here, see Fig. 8.

Our goal to introduce the results with strong Allee effect here is purely motivational and as a conduit for future investigations. We refrain from the mathematical analysis of the strong Allee effect presently, and relegate it for detailed future work. Note current works in this vein, that consider strong Allee effects in TYC context (Bhattacharyya et al., 2020; Beauregard et al., 2020), only find hyperbolic extinction boundaries, but this is probably due to the parameter choices of simulations therein. This begets the question of how in general does the extinction boundary look in mating models, with the inclusion of Allee effects, which seems to be an open problem in ecology (Berec, 2004). For systems that are monotone, say of competitive or cooperative type, there is a large body of results, see (Schreiber, 2004; Jiang and Shi, 2009; Smith and Thieme, 2001; Hirsch and Smith, 2006; Jiang et al., 2004) and the references within, that point to the hyperbolic shape of the threshold manifold. However, the systems we consider are non-monotone (easily observed by checking the signs of the off-diagonal terms of the jacobian matrix) - and the threshold boundary for such systems is less investigated.

Our other result concerns the stopping of harvesting or stocking, at various finite times, and initial densities of the wild-type, so as to still yield extinction. This is elucidated via Figs. 4 - 5. Lastly, we would like to comment on our results concerning spatial/Turing instability. Here again, we see via Lemma 11 and Theorem 4, that the FHMS system cannot produce Turing patterns, whereas the FHMS system with weak Allee effect can. Thus the weak Allee effect can cause the population of males and females to spread patchily in space. This has been observed elsewhere in the literature as well (Parshad et al., 2016a,b).

Acknowledgements

ET and RP would like to acknowledge valuable support from the National Science Foundation via DMS 1839993. MB would like to acknowledge valuable support from the National Science Foundation via DMS 1715044. JB is supported by the grants from Science and Engineering Research Board (SERB), Govt. of India (File No. TAR/2018/000283).

Conflict of interest

The authors declare that they have no conflict of interest.

References

- Alonzo SH, Mangel M (2004) The effects of size-selective fisheries on the stock dynamics of and sperm limitation in sex-changing fish. *Fishery Bulletin* 102(1):1–13
- Beauregard MA, Parshad RD, Boon S, Conaway H, Griffin T, Lyu J (2020) Optimal control and analysis of a modified trojan y-chromosome strategy. *Ecological Modelling* 416:108854

- Berec L (2004) Mathematical modeling in ecology and epidemiology. HIV/AIDS modeling and control, automatic
- Bhattacharyya J, Roelke DL, Walton JR, Banerjee S (2020) Using yy supermales to destabilize invasive fish populations. *Theoretical Population Biology*
- Boukal DS, Berec L (2002) Single-species models of the allee effect: extinction boundaries, sex ratios and mate encounters. *Journal of Theoretical Biology* 218(3):375–394
- Britton J, Gozlan RE, Copp GH (2011) Managing non-native fish in the environment. *Fish and fisheries* 12(3):256–274
- Courchamp F, Clutton-Brock T, Grenfell B (1999) Inverse density dependence and the allee effect. *Trends in ecology & evolution* 14(10):405–410
- Courchamp F, Berec L, Gascoigne J (2008) Allee effects in ecology and conservation. Oxford University Press
- Gutierrez JB, Teem JL (2006) A model describing the effect of sex-reversed yy fish in an established wild population: the use of a trojan y chromosome to cause extinction of an introduced exotic species. *Journal of Theoretical Biology* 241(2):333–341
- Gutierrez JB, Hurdal MK, Parshad RD, Teem JL (2012) Analysis of the trojan y chromosome model for eradication of invasive species in a dendritic riverine system. *Journal of Mathematical Biology* 64(1-2):319–340
- Gutierrez JB, Kouachi S, Parshad RD (2013) Global existence and asymptotic behavior of a model for biological control of invasive species via supermale introduction. *Communications in Mathematical Sciences* 11(4):971–992
- Havel JE, Kovalenko KE, Thomaz SM, Amalfitano S, Kats LB (2015a) Aquatic invasive species: challenges for the future. *Hydrobiologia* 750(1):147–170
- Havel JE, Kovalenko KE, Thomaz SM, Amalfitano S, Kats LB (2015b) Aquatic invasive species: challenges for the future. *Hydrobiologia* 750(1):147–170
- Hirsch MW, Smith H (2006) Monotone dynamical systems. In: *Handbook of differential equations: ordinary differential equations*, vol 2, Elsevier, pp 239–357
- Jiang J, Shi J (2009) Bistability dynamics in structured ecological models. *Spatial Ecology*, in: Chapman & Hall/CRC Math Comput Biol Ser pp 33–62
- Jiang J, Liang X, Zhao XQ (2004) Saddle-point behavior for monotone semiflows and reaction–diffusion models. *Journal of Differential Equations* 203(2):313–330
- Liu H, Guan B, Xu J, Hou C, Tian H, Chen H (2013) Genetic manipulation of sex ratio for the large-scale breeding of yy super-male and xy all-male yellow catfish (*pelteobagrus fulvidraco* (richardson)). *Marine biotechnology* 15(3):321–328
- Lyu J (2018) *Mathematical Methods in Invasive Species Control*. Clarkson University
- Lyu J, Schofield PJ, Reaver KM, Beauregard M, Parshad RD (2020) A comparison of the trojan y chromosome strategy to harvesting models for eradication of nonnative species. *Natural Resource Modeling* 33(2): p e12252
- Mair G, Abucay J, Abella T, Beardmore J, Skibinski D (1997) Genetic manipulation of sex ratio for the large-scale production of all-male tilapia *oreochromis niloticus*. *Canadian Journal of Fisheries and Aquatic Sciences* 54(2):396–404
- Murray J (2001) *Mathematical biology II: spatial models and biomedical applications*. Springer New York
- Myers JH, Simberloff D, Kuris AM, Carey JR (2000) Eradication revisited: dealing with exotic species. *Trends in ecology & evolution* 15(8):316–320
- Neuenhoff RD, Swain DP, Cox SP, McAllister MK, Trites AW, Walters CJ, Hammill MO (2019) Continued decline of a collapsed population of atlantic cod (*gadus morhua*) due to predation-driven allee effects. *Canadian Journal of Fisheries and Aquatic Sciences* 76(1):168–184
- Okubo, A., & Levin, S. A. (2013). *Diffusion and ecological problems: modern perspectives* (Vol. 14). Springer Science & Business Media.
- Palkovacs EP, Moritsch MM, Contolini GM, Pelletier F (2018) Ecology of harvest-driven trait changes and implications for ecosystem management. *Frontiers in Ecology and the Environment* 16(1):20–28
- Parshad RD (2011) Long time behavior of a pde model for invasive species control. *International Journal of Mathematical Analysis*
- Parshad RD, Gutierrez JB (2010) On the well posedness and refined estimates for the global attractor of the tyt model. *Boundary Value Problems* 2010:1–29
- Parshad RD, Gutierrez JB (2011) On the global attractor of the trojan y chromosome model. *Communications on Pure & Applied Analysis* 10(1):339
- Parshad RD, Quansah E, Black K, Beauregard M (2016a) Biological control via ecological damping: an approach that attenuates non-target effects. *Mathematical biosciences* 273:23–44

- Parshad RD, Quansah E, Black K, Upadhyay RK, Tiwari S, Kumari N (2016b) Long time dynamics of a three-species food chain model with allee effect in the top predator. *Computers & Mathematics with Applications* 71(2):503–528
- Parshad RD, Beauregard MA, Takyi EM, Griffin T, Bobo L (2019) Large and small data blow-up solutions in the trojan y chromosome model. *arXiv preprint (unpublished) arXiv:190706079*
- Perälä T, Kuparinen A (2017) Detection of allee effects in marine fishes: analytical biases generated by data availability and model selection. *Proceedings of the Royal Society B: Biological Sciences* 284(1861):20171284
- Perko L (2013) *Differential equations and dynamical systems*, vol 7. Springer Science & Business Media
- Perrin N (2009) Sex reversal: a fountain of youth for sex chromosomes? *Evolution: International Journal of Organic Evolution* 63(12):3043–3049
- Schill DJ, Heindel JA, Campbell MR, Meyer KA, Mamer ER (2016a) Production of a yy male brook trout broodstock for potential eradication of undesired brook trout populations. *North American Journal of Aquaculture* 78(1):72–83
- Schreiber S (2004) On allee effects in structured populations. *Proceedings of the American Mathematical Society* 132(10):3047–3053
- Scott A, Penman D, Beardmore J, Skibinski D (1989) The yysupermale in *oreochromis niloticus* (l.) and its potential in aquaculture. *Aquaculture* 78(3-4):237–251
- Smith H, Thieme H (2001) Stable coexistence and bi-stability for competitive systems on ordered banach spaces. *Journal of Differential Equations* 176(1):195–222
- Stephens PA, Sutherland WJ (1999) Consequences of the allee effect for behaviour, ecology and conservation. *Trends in ecology & evolution* 14(10):401–405
- Teem JL, Gutierrez JB, Parshad RD (2014) A comparison of the trojan y chromosome and daughterless carp eradication strategies. *Biological invasions* 16(6):1217–1230
- Vera Cruz E, Mair G, Marino R (1999) *Feminization of genotypically yy-nile tilapia, oreochromis niloticus*. PCAMRD Book Series (Philippines)
- Wang X, Walton JR, Parshad RD, Storey K, Boggess M (2014) Analysis of the trojan y-chromosome eradication strategy for an invasive species. *Journal of mathematical biology* 68(7):1731–1756
- Wang X, Walton JR, Parshad RD (2016) Stochastic models for the trojan y-chromosome eradication strategy of an invasive species. *Journal of biological dynamics* 10(1):179–199
- Wedekind C (2012) Managing population sex ratios in conservation practice: how and why. *Topics in conservation biology* pp 81–96
- Zhao X, Liu B, Duan N (2012) Existence of global attractor for the trojan y chromosome model. *Electronic Journal of Qualitative Theory of Differential Equations* 2012(36):1–16

Appendix A Stability analysis for FHMS model without weak Allee effect

The system (3) has the nullclines $F_i = 0$ ($i = 1, 2$). Solving these nullclines yields the following equilibria:

- (i) Invasive fish-free equilibrium $E_0 = (0, 0)$ exists always and is locally asymptotically stable (as $s < 1$).
- (ii) coexistence equilibria $E_i^* = (f_i^*, \mu f_i^*)$, where $\mu = \frac{(1-r)(1+h)}{r(1-s)}$ and

$$f_i^* = \frac{1}{2(1+\mu)} \left\{ 1 \pm \sqrt{1 - \frac{4(1+\mu)(1+h)}{r\alpha\mu}} \right\}, \quad (i = 1, 2).$$

The following lemma gives the conditions for existence of the unique interior equilibrium E_i^* ($i = 1, 2$):

Lemma 12 . *The interior equilibrium E_i^* of the system (3) exists if either one of the following two conditions holds:*

- (i) $s \geq s^*$ and $h_* < h < h^*$;
- (ii) $0 \leq h \leq h_*$ and $\alpha > \frac{4}{r(1-r)}$, where $s^* = \frac{1}{r} + \left(\frac{1-r}{4}\right) \left(\frac{4h}{r} - \alpha\right)$, $h_* = \frac{r}{4} \left\{ \alpha - \frac{4}{r(1-r)} \right\}$ and $h^* = \frac{r}{4} \left(\alpha - \frac{4}{r} \right)$.

The linearized system of (3) about an equilibrium \hat{E} is given by $\frac{dX}{dt} = J(\hat{E})X$, where $X = (f \ m)^T$ and $J(\hat{E})$ is the Jacobian matrix of the system (3) evaluated at \hat{E} . We analyze the stability of system (3) by using eigenvalue analysis of the Jacobian matrix evaluated at the appropriate equilibrium. At E_0 , the eigenvalues of the Jacobian matrix of the system (3) are $s - 1$ and $-(1 + h)$. Since $0 \leq s < 1$, all the eigenvalues of the Jacobian matrix $J(E_0)$ are negative. This gives the following lemma:

Lemma 13 . *The invasive fish-free equilibrium E_0 is always locally asymptotically stable.*

The Jacobian of the system (3) evaluated at E_i^* is given by

$$J_i^* = \begin{pmatrix} -r\alpha\mu f_i^{*2} & r\alpha f_i^*(1 - f_i^* - 2\mu f_i^*) \\ (1-r)\alpha\mu f_i^*(1 - 2f_i^* - \mu f_i^*) & -(1-r)\alpha\mu f_i^{*2} \end{pmatrix}.$$

We have $\text{Tr}(J_i^*) = -\alpha\mu f_i^{*2} < 0$ and $\text{Det}(J_i^*) = -r(1-r)\alpha^2\mu f_i^{*2} \{1 - 2(1+\mu)f_i^*\} \{1 - (1+\mu)f_i^*\}$. Therefore, the system (3) is locally asymptotically stable at E_i^* if and only if $\text{Det}(J_i^*) > 0$. This gives the following lemma:

Lemma 14 . Assume that the conditions of Lemma 12 are satisfied. If $\frac{r(1-s)}{2\{1+h-r(h+s)\}} < f_i^* < \frac{r(1-s)}{1+h-r(h+s)}$ holds, then the system (3) is locally asymptotically stable at E_i^* .

Appendix B FHMS with weak allee

B.1 Proof of boundedness of FHMS model with weak Allee effect (6)

Proof . Case (i):

Let $0 \leq f(0) < 1$. If possible, let there exists $t > 0$ such that $f(t) \geq 1$. We define $t_0 = \min\{t : f(t) \geq 1\}$. Then $f(t_0) = 1$ and $f(t) < 1$ for $0 \leq t < t_0$. Now, we have $f'(t_0) = -r\alpha m^2(t_0) - (1+h) < 0$. By the continuity of $f'(t)$, there exists $\delta > 0$ such that $f'(t) < 0$ for all $t \in (t_0 - \delta, t_0 + \delta)$.

Let $t_1 = t_0 - \frac{\delta}{2}$. Then $t_0 - \delta < t_1 < t_0 < t_0 + \delta$. Since $f(t)$ is strictly decreasing function for all $t \in (t_0 - \delta, t_0 + \delta)$, we have $f(t_1) > f(t_0) = 1$ which contradicts to the definition of t_0 . Therefore, we can conclude that $f(t) \geq 1$ cannot be true for any $t > 0$ when $0 \leq f(0) < 1$.

Case (ii):

Let $f(0) \geq 1$. We first assume that $f(0) = 1$. Then $f'(0) = -r\alpha m^2(0) - (1+h) < 0$ and so, there exists $\delta_0 > 0$ such that $f'(t) < 0$ for all $t \in [0, \delta_0)$. Therefore, for all $t > \delta_0$, we have $f(t) < f(\delta_0) < f(0) = 1$.

Next assume that $f(0) > 1$. Then $f'(0) < 0$ implies there exists $\delta_1 > 0$ such that $f'(t) < 0$ for all $t \in [0, \delta_1)$. Since $f'(t)$ is strictly decreasing for all $t \in [0, \delta_1)$, it follows that $f(\delta_1) < f(0)$. Suppose that there exists $t > \delta_1$ such that $f(t) > f(0)$. Let $t_2 > \delta_1$ be defined by $t_2 = \min\{t > \delta_1 : f(t) > f(0)\}$. Then $f(t_2) > f(0) > 1$ implies $f'(t_2) = r\alpha f^2(t_2)m(t_2)(1 - f(t_2) - m(t_2)) - (1+h)f(t_2) < 0$ and so, there exists $\delta_2 > 0$ such that $f'(t) < 0$ for all $t \in (t_2 - \delta_2, t_2 + \delta_2)$.

One now sees that $f'(t_2 - \frac{\delta_2}{2}) < 0$ from which it follows that $f(t_2 - \frac{\delta_2}{2}) > f(t_2) > f(0) > 1$, contradicting to the definition of t_2 . Therefore, for $f(0) \geq 1$, there cannot exist $t > t_2$ such that $f(t) > f(0)$. Hence, all the solutions of the system (6) are contained in some bounded subset in the first quadrant of the fm -plane.

B.2 Proof of saddle-node bifurcation in FHMS with weak Allee effect (6)

Proof . Solving $G(g) = 0 = G'(f)$ we see that the equation $G(f) = 0$ has a double root $\frac{2}{3(1+\mu)}$ satisfying $G''\left(\frac{2}{3(1+\mu)}\right) = \frac{4}{(1+\mu)} \neq 0$. The two nontrivial nullclines $\phi_i(f, m) = 0$ ($i = 1, 2$) intersect at the instantaneous interior equilibrium $E^* = \left(\frac{2}{3(1+\mu)}, \frac{2\mu}{3(1+\mu)}\right)$. At E^* , the slopes of $\phi_i(f, m) = 0$ ($i = 1, 2$) are equal and so $\frac{\bar{F}_{1f}}{\bar{F}_{1m}} = \frac{\bar{F}_{2f}}{\bar{F}_{2m}}$, which gives $\text{Det}(J^*) = 0$. Solving $\text{Det}(J^*) = 0$, the critical value of h , say, $h = h^*$ can be obtained. At $h = h^*$, if $\text{Tr}(J^*) \neq 0$, then the Jacobian of the system (6) has a simple zero eigenvalue.

Let $\bar{F}(f, m; s) = (\bar{F}_1 \ \bar{F}_2)^T$ and V^* and W^* are eigenvectors corresponding to the zero eigenvalue for $J^*|_{h=h^*}$ and $J^{*T}|_{h=h^*}$ respectively. We obtain $\bar{F}_h(f, m; h) = \left(\frac{-2}{3(1+\mu)}, 0\right)^T$, $U^* = (1 \ \mu)^T$ and $V^* = \left(1 \ \frac{3r(1-\mu)}{4(1-r)\mu}\right)^T$ so that $V^{*T}\bar{F}_h(E^*; h^*) = \frac{-2}{3(1+\mu)}$ and $V^{*T}(D\bar{F}_h)(U^*) = -1$.

Due to the complexity in the algebraic expressions involved, we will use numerical simulations to verify $V^{*T}[D^2\bar{F}(E^*; h^*)(U^*, U^*)] \neq 0$. Under these conditions, the system (6) satisfies Sotomayor's theorem for a saddle-node bifurcation at E^* when h crosses h^* . This gives the following lemma.

Keeping all parameters fixed and varying the harvesting parameter h we observe that the coexisting equilibria E_i^* ($i = 1, 2$) collide to each other, generating a unique instantaneous interior equilibrium. From Fig. 2(b), it is

observed that the interior equilibria E_i^* ($i = 1, 2$) cease to exist when h is increased through $h^* = 0.4$. At $h = 0.4$, we have $E^* = (0.2, 0.47)$ ($i = 1, 2$) and

$$J_i^* = \begin{pmatrix} 0.56 & -0.24 \\ 1.96 & -0.84 \end{pmatrix}$$

has a simple zero eigenvalue. Also, we obtain $U^* = (1 \ 2.33)^T$, $V^* = (1 \ -0.286)^T$, $V^{*T} \bar{F}_h(E^*; h^*) = -0.2$, $V^{*T}(DF_h)(U^*) = -1$ and $V^{*T}[D^2\bar{F}(E^*; h^*)(U^*, U^*)] = -29.997$, satisfying the conditions of a saddle-node bifurcation at E^* when h crosses $h = h^*$.

B.3 Proof of Hopf bifurcation in FHMS system with weak Allee effect (6)

Proof. We consider the following parameter set $r = 0.5, \alpha = 90, h = 0.24, s = 0.59317665$. Then $E_1^* = (0.16534, 0.50397)$ is an interior equilibrium. Evaluating the Jacobian of system (6) at E_1^* , we obtain

$$J_i^* = \begin{pmatrix} 0.62 & -0.21318 \\ 1.86 & -0.62 \end{pmatrix}. \quad (17)$$

The corresponding eigenvalues are given as $\lambda_{1,2} = \pm 0.11005i$. Clearly, the trace and determinant of Eqn. (17) is 0 and $0.01211 > 0$ respectively. Now, referencing the Jacobian of system (6) again, let $\mu = \frac{\lambda}{(1-s)}$ where $\lambda = \frac{(1-r)(1+h)}{r}$. Then

$$\frac{d}{ds}(\text{Tr}(J_i^*)) = \frac{\lambda r \alpha f_i^{*2}}{(1-s)^2} \left(1 - f_i^* \left(1 + \frac{1}{r} + \frac{2\lambda}{(1-s)} \right) \right). \quad (18)$$

Now, $\frac{d}{ds}(\text{Tr}(J_i^*))|_{E_1^*} = -4.6446 \neq 0$ at $s=0.59317665$. Hence, the FHMS model with weak Allee effect undergoes a Hopf bifurcation with respect to the bifurcation parameter $s = s_{hf} = 0.59317665$.

We now vary the stocking rate s . As seen in Fig. 7, when $s = 0.59318$, the interior equilibrium $E_1^* = (0.16531, 0.50388)$ is a spiral source. The eigenvalues associated to E_1^* are $\lambda_1 = 0.00033529 + 0.10753i$ and $\lambda_2 = 0.00033529 - 0.10753i$. When the stocking rate is decreased to $s = 0.59316$, $E_1^* = (0.16548, 0.50436)$ gains stability and becomes a spiral sink. It's associated eigenvalues are $\lambda_1 = -0.0014934 + 0.12056i$ and $\lambda_2 = -0.0014934 - 0.12056i$. Clearly, the pair of complex conjugate eigenvalues cross the imaginary axis of the complex plane when the stocking rate s decreases from $s = 0.59318$ to $s = 0.59316$. This leads to a subcritical Hopf bifurcation which gives rise to an unstable limit cycle.